Analysis and Comparison of Dynamic Models for the Doubly Fed Induction Generator Wind Turbine

YIN Ming, LI Gengyin, ZHOU Ming, ZHAO Chengyong

(Key Laboratory of Power System Protection and Dynamic Security Monitoring and Control Under Ministry of Education, North China Electric Power University, Baoding 071003, China)

Abstract: Doubly fed induction generator (DFIG) wind turbines are widely utilized in large wind plants. Research of the dynamic behaviors of DFIG wind turbine is of great importance. In this paper, the 8th, 5th and 3rd order models of DFIG wind turbines are discussed respectively. The 8th order model includes the complete drive train, the stator and the rotor models. The 5th order model contains the stator and the rotor models, as well as a reduced drive train model. The 3rd order model, with the stator transients being neglected, comprises the rotor model and a reduced drive train model. These three types of DFIG wind turbine are modeled in MATLAB/Simulink software package. Two cases of simulation are conducted to verify the models and compare their responses. The simulation results demonstrate that the 8th order model is the most precise model, but needs the longest simulation time; the 3rd order model is a good approximation and the most time-effective; the 5th order model is suitable for most studies that require both fast computation speed and relatively high precision.

This work is supported by National Natural Science Foundation of China (No. 50577018).

Key words: doubly fed induction generator(DFIG); wind generation; dynamic models; variable speed wind turbine

CLC number: TM614

0 Introduction

Due to its renewable nature, increasingly competitive cost, and environmental friendliness, wind generation is among the best technologies available today to provide a sustainable energy supply to the world development. Globally, the total installed capacity of the wind turbines has reached as much as 39.234 GW by 2003 and will exceed 110 GW by 2012[1]. In China, the wind market has picked up pace with the installed capacity increasing from 0.746 GW by 2004 to 30 GW by 2020. As penetration of wind energy increases, the dynamic characteristics of wind turbines become increasingly important to the power grids that they are connected to[2].

Today, doubly fed induction generator (DFIG) wind turbines have been proved as a promising technology and are widely utilized due to their distinct advantages over other types of wind turbine[3]. In order to investigate the impacts of large scale of DFIG installations on the operation and control of power systems, accurate models are required indeed. Till now, some meaningful studies have been made on the modeling of wind turbine[4-10]. For various study purposes, different order wind turbine models should be applied. In the paper, the 8th, 5th and 3rd order models of DFIG wind turbine are discussed. The 8th model includes the stator and the rotor dynamics as well as the mechanical dynamics. The 5th model simplifies the mechanical dynamics. The 3rd model neglects the stator transients and only considers the rotor transients. Three types of DFIG wind turbines are modeled in MATLAB/Simulink software package. Simulation cases are also performed to verify these models and compare their responses.

收稿日期: 2005-12-23; 修回日期: 2006-01-22。
国家自然科学基金资助项目(50577018)。

1 Dynamic Models of DFIG Wind Turbine

1.1 Model of Wind Turbine

The amount of aerodynamic power production is related to wind speeds as follows[11]:

$$P_W = 0.5\rho\pi R^2 v^3 C_P(\theta,\gamma) \quad (1)$$

where, ρ is the air density; R is the wind turbine radius; v is the wind speed; C_P is the power coefficient; θ is the pitch angle; $\gamma=\omega_W R/v$ is the tip speed ratio (TSR), and ω_W is the turbine rotor speed.

The output aerodynamic torque is given by the following equation:

$$T_W = \frac{0.5\rho\pi R^3 v^2 C_P(\theta,\gamma)}{\gamma} \quad (2)$$

When the power generation is less than the rated power, the wind turbine will be expected to extract as much wind power as possible. After the rated power is reached, the blades are pitched to reduce the power coefficient C_p and thereby to keep the rated power. In this process, the rotor speed will have an obvious lift to absorb and store the surplus wind power[12].

1.2 Model of Drive Train

The drive train of DFIG consists of five parts, viz, rotor, low-speed shaft, gearbox, high-speed shaft and generator. In the analysis, other parts of wind turbines,

e. g. tower and flap bending modes can be reasonably neglected. The basic structure of the drive train is depicted in Fig. 1.

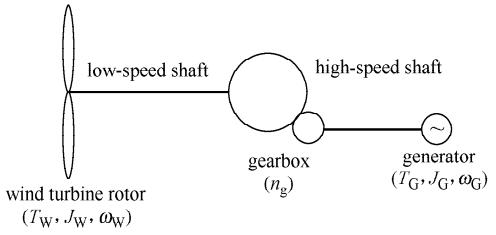

Fig. 1 Basic structure of the drive train

References [8-9] propose three-lumped mass and two-lumped mass methods respectively for analyzing the drive train. In this paper the two-lumped mass method is applied due to its efficiency and convenience. The analysis is referred to the high-speed side. Taken the relationship between the twist angle and the mechanical angular speed into account, the dynamics of the drive train system can be expressed by the following equation[13]:

$$\begin{cases} \dfrac{\mathrm{d}\theta_G}{\mathrm{d}t} = \omega_G \\ \dfrac{\mathrm{d}\omega_G}{\mathrm{d}t} = \dfrac{T_G - \delta_G\omega_G + k(\theta_W - \theta_G)}{J_G} \\ \dfrac{\mathrm{d}\theta_W}{\mathrm{d}t} = \omega_W \\ \dfrac{\mathrm{d}\omega_W}{\mathrm{d}t} = \dfrac{T_W - \delta_W\omega_W - k(\theta_W - \theta_G)}{J_W} \end{cases} \tag{3}$$

where, the subscripts "W" and "G" represent the parameters of the turbine side and the generator side respectively; J is the rotating inertia of the equivalent lumped masses; n_g is the gear ratio; δ is the rotating damping; T is the torque; θ is the twist angle; k is the shaft stiffness; ω is the mechanical angular speed.

1.3 Model of DFIG

The dynamic models of DFIG are derived from the two-phase synchronous reference frame. In the following analysis, the motor convention is applied.

The electrical model of DFIG in the synchronous reference frame is given in equations (4) and (5), where the quantities on the rotor side have been referred to the stator side. The model includes two sets of equations, i. e. one is the voltage equations given by equation (4) and the other is the flux equations expressed by equation (5)[14].

$$\begin{cases} u_{ds} = R_s i_{ds} + \dfrac{\mathrm{d}\psi_{ds}}{\mathrm{d}t} - \omega_s\psi_{qs} \\ u_{qs} = R_s i_{qs} + \dfrac{\mathrm{d}\psi_{qs}}{\mathrm{d}t} + \omega_s\psi_{ds} \\ u_{dr} = R_r i_{dr} + \dfrac{\mathrm{d}\psi_{dr}}{\mathrm{d}t} - (\omega_s - \omega_r)\psi_{qr} \\ u_{qr} = R_r i_{qr} + \dfrac{\mathrm{d}\psi_{qr}}{\mathrm{d}t} + (\omega_s - \omega_r)\psi_{dr} \end{cases} \tag{4}$$

$$\begin{cases} \psi_{ds} = (L_{sk} + L_m)i_{ds} + L_m i_{dr} \\ \psi_{qs} = (L_{sk} + L_m)i_{qs} + L_m i_{qr} \\ \psi_{dr} = (L_{rk} + L_m)i_{dr} + L_m i_{ds} \\ \psi_{qr} = (L_{rk} + L_m)i_{qr} + L_m i_{qs} \end{cases} \tag{5}$$

where, u and i are the voltage and current respectively; ψ is the flux linkage; R is the winding resistance; L_k is the leakage inductance; L_m is the mutual inductance; ω is the electrical angular speed; subscripts "s" and "r" refer to the stator and rotor side respectively; subscripts "d" and "q" refer to the d-axis and q-axis respectively.

The electromagnetic torque is given by

$$T_G = \frac{3}{2}n_p L_m(i_{qs}i_{dr} - i_{ds}i_{qr}) \tag{6}$$

where, n_p is the number of pole pairs.

According to equations (4) and (5), the equivalent circuits of the dq-model in the synchronous reference frame are envisaged in Fig. 2.

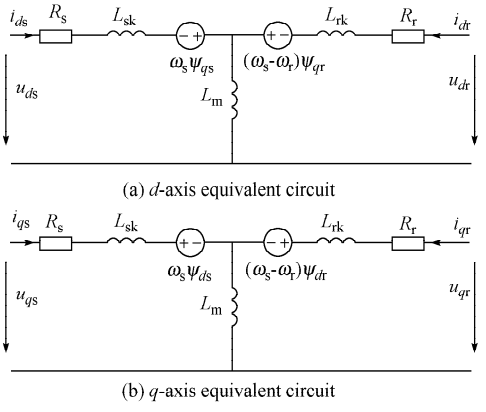

Fig. 2 Equivalent circuits of DFIG in the synchronous frame

Provided equation (5) is introduced into equation (4), equation (7) is then obtained. It reveals the electromagnetic dynamic performances of DFIG.

$$m\frac{\mathrm{d}}{\mathrm{d}t}\begin{bmatrix} i_{ds} \\ i_{qs} \\ i_{dr} \\ i_{qr} \end{bmatrix} = \begin{bmatrix} a & b & -c & -d \\ -b & a & d & -c \\ -e & f & g & -h \\ -f & -e & h & g \end{bmatrix}\begin{bmatrix} i_{ds} \\ i_{qs} \\ i_{dr} \\ i_{qr} \end{bmatrix} + \begin{bmatrix} -L_r & 0 & L_m & 0 \\ 0 & -L_r & 0 & L_m \\ L_m & 0 & -L_s & 0 \\ 0 & L_m & 0 & -L_s \end{bmatrix}\begin{bmatrix} u_{ds} \\ u_{qs} \\ u_{dr} \\ u_{qr} \end{bmatrix} \tag{7}$$

where, $L_s = L_{sk} + L_m$, $L_r = L_{rk} + L_m$, $m = L_m^2 - L_r L_s$, $a = R_s L_r$, $b = (\omega_s - \omega_r)L_m^2 - \omega_s L_s L_r$, $c = R_r L_m$, $d = \omega_r L_m L_r$, $e = R_s L_m$, $f = \omega_r L_m L_s$, $g = R_r L_s$, $h = (\omega_s - \omega_r)L_s L_r - \omega_s L_m^2$.

2 DFIG Wind Turbine Models with Different Orders

In practice, different ordered DFIG wind turbine models are used when the study focuses are different. In this section, the purpose and structure of 8th, 5th and 3rd order models will be discussed.

2.1 The 8th Order Model of DFIG Wind Turbine

Some problems, e. g. those concerning mechanical performances of wind turbines, mechanical dynamics of the

drive train need to be accurately simulated. In this scenario, the drive train has to be considered as a two-lumped mass quantity that is defined by equation (3). Electrically, the model of generator has to include all the dynamics from both the stator and the rotor. So, the 8th order model of DFIG, based on equation (3) and equation (7), is acquired.

2.2 The 5th Order Model of DFIG Wind Turbines

However, the 8th order model is not required for all studies. When the electrical characteristics or torsion-related problems are the main interest, the drive train can be reduced to a single equivalent lumped mass, which is defined by the following equation:

$$J_{\mathrm{eq}} = J_{\mathrm{G}} + \frac{J_{\mathrm{W}}}{n_{\mathrm{g}}^2} \tag{8}$$

where, n_{g} is the gearbox ratio.

The drive train dynamics, therefore, can be described as[14]:

$$J_{\mathrm{eq}} \frac{\mathrm{d}\omega_{\mathrm{G}}}{\mathrm{d}t} = T_{\mathrm{W}} - T_{\mathrm{G}} - D\omega_{\mathrm{G}} \tag{9}$$

where, D is the friction coefficient.

On the rotor side, two angular speeds (the electrical angular speed ω_{r} and the mechanical angular speed ω_{G}) exist and they have such a relationship as:

$$\omega_{\mathrm{r}} = n_{\mathrm{p}}\omega_{\mathrm{G}} \tag{10}$$

Introduce equations (6), (8) and (10) into equation (9) and then the drive train model is:

$$J_{\mathrm{eq}} \frac{\mathrm{d}\omega_{\mathrm{r}}}{\mathrm{d}t} = n_{\mathrm{p}}[T_{\mathrm{W}} - 1.5 n_{\mathrm{p}} L_{\mathrm{m}}(i_{qs} i_{dr} - i_{ds} i_{qr}) - D\omega_{\mathrm{r}}] \tag{11}$$

So, equations (7) and (11) constitute the 5th order model of DFIG wind turbines.

2.3 The 3rd Order Model of DFIG Wind Turbines

When the transients in the stator of the DFIG and in the power system are considered, the order of the simulated system will be overwhelmingly augmented and be extremely time consuming. In this case, the order of the generator model should be further reduced. For the electromagnetic behaviors in the stator are much faster than those in the rotor and have little effect on the machine's transient stability, it can be neglected for the stability study[7], which means the derivatives of the stator flux in equation (4) become zeros. So, equation (4) can be changed into the following form:

$$\begin{cases} u_{ds} = R_{\mathrm{s}} i_{ds} - \omega_{\mathrm{s}} \psi_{qs} \\ u_{qs} = R_{\mathrm{s}} i_{qs} + \omega_{\mathrm{s}} \psi_{ds} \\ u_{dr} = R_{\mathrm{r}} i_{dr} + \dfrac{\mathrm{d}\psi_{dr}}{\mathrm{d}t} - (\omega_{\mathrm{s}} - \omega_{\mathrm{r}})\psi_{qr} \\ u_{qr} = R_{\mathrm{r}} i_{qr} + \dfrac{\mathrm{d}\psi_{qr}}{\mathrm{d}t} + (\omega_{\mathrm{s}} - \omega_{\mathrm{r}})\psi_{dr} \end{cases} \tag{12}$$

According to the first two equations in both equation (5) and equation (12), the d- and q-components of the rotor current i_{dr} and i_{qr} can be expressed with u_{ds}, u_{qs}, i_{ds} and i_{qs} as follows:

$$\begin{cases} i_{dr} = \dfrac{R_{\mathrm{s}} i_{ds} - \omega_{\mathrm{s}} L_{\mathrm{s}} i_{qs} - u_{ds}}{\omega_{\mathrm{s}} L_{\mathrm{m}}} \\ i_{qr} = \dfrac{R_{\mathrm{s}} i_{qs} + \omega_{\mathrm{s}} L_{\mathrm{s}} i_{ds} - u_{qs}}{\omega_{\mathrm{s}} L_{\mathrm{m}}} \end{cases} \tag{13}$$

Two electrical potential components e_d and e_q are defined as follows:

$$\begin{cases} e_d = -\dfrac{\omega_{\mathrm{s}} L_{\mathrm{m}} \psi_{qr}}{L_{\mathrm{r}}} \\ e_q = \dfrac{\omega_{\mathrm{s}} L_{\mathrm{m}} \psi_{dr}}{L_{\mathrm{r}}} \end{cases} \tag{14}$$

Introduce the last two equations in equtions (5) and (13) into equation (14) and then the stator current in terms of the d- and q-components i_{ds} and i_{qs} can be expressed by e_d, e_q, u_{ds} and u_{qs}.

Meanwhile, the other two voltage components u_{dr}^* and u_{qr}^* are defined as follows:

$$\begin{cases} u_{dr}^* = -\dfrac{\omega_{\mathrm{s}} L_{\mathrm{m}} u_{qr}}{L_{\mathrm{r}}} \\ u_{qr}^* = \dfrac{\omega_{\mathrm{s}} L_{\mathrm{m}} u_{dr}}{L_{\mathrm{r}}} \end{cases} \tag{15}$$

Introduce equations (14) and (15) into equation (12) and then the following equations are obtained:

$$\frac{\mathrm{d}}{\mathrm{d}t}\begin{bmatrix} e_d \\ e_q \end{bmatrix} = -\begin{bmatrix} \dfrac{R_{\mathrm{r}}}{L_{\mathrm{r}}} & -(\omega_{\mathrm{s}} - \omega_{\mathrm{r}}) \\ \omega_{\mathrm{s}} - \omega_{\mathrm{r}} & \dfrac{R_{\mathrm{r}}}{L_{\mathrm{r}}} \end{bmatrix}\begin{bmatrix} e_d \\ e_q \end{bmatrix} + \begin{bmatrix} u_{dr}^* \\ u_{qr}^* \end{bmatrix} + \begin{bmatrix} -\dfrac{\omega_{\mathrm{s}} R_{\mathrm{r}} L_{\mathrm{m}}^2}{L_{\mathrm{r}}^2} i_{qs} \\ \dfrac{\omega_{\mathrm{s}} R_{\mathrm{r}} L_{\mathrm{m}}^2}{L_{\mathrm{r}}^2} i_{ds} \end{bmatrix} \tag{16}$$

The electromagnetic torque is given as:

$$T_{\mathrm{G}} = \frac{3}{2} \frac{u_{qs} i_{qs} + u_{ds} i_{ds}}{\omega_{\mathrm{s}}} \tag{17}$$

Therefore, equations (9), (10), (14), (16) and (17) constitute the 3rd order model of DFIG wind turbine.

3 Simulink Based Modeling

The three types of DFIG wind turbine model are developed in MATLAB/Simulink R14 software package. Each type of model consists of two blocks: the drive train block "DriveTr" and the generator block "Generator". The overall structures of the 8th and the 5th order models of DFIG wind turbine are shown in Fig. 3. As shown in the figure, the d-and q-components of the stator and rotor currents i_{ds}, i_{qs}, i_{dr} and i_{qr} are outputted from "Generator" and passed to "DriveTr" to make the electromagnetic torque T_{G}. The input mechanical torque T_{W} is determined by equation (2).

The generator block "Generator" in the 8th and the 5th order DFIG wind turbine are both derived from equation (7) and are represented by Fig. 4. In the figure, the gains a, c, e, g have the same meaning as those defined in equation (7)

and the user-defined functions $f_1(u) \sim f_8(u)$ are used to calculate b, $-d$, $-b$, d, f, $-h$, $-f$ and h respectively. The user-defined function "$u_s\_u_r$" is used to calculate the input terms in equation (7). The blocks "Cal_i_{ds}, Cal_i_{qs}, Cal_i_{dr} and Cal_i_{qr}" are the integrator blocks.

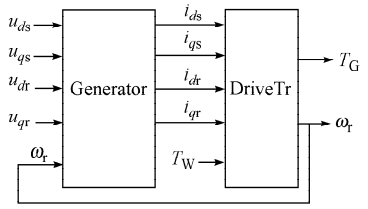

Fig. 3 Overall structure of the 8th and 5th order models

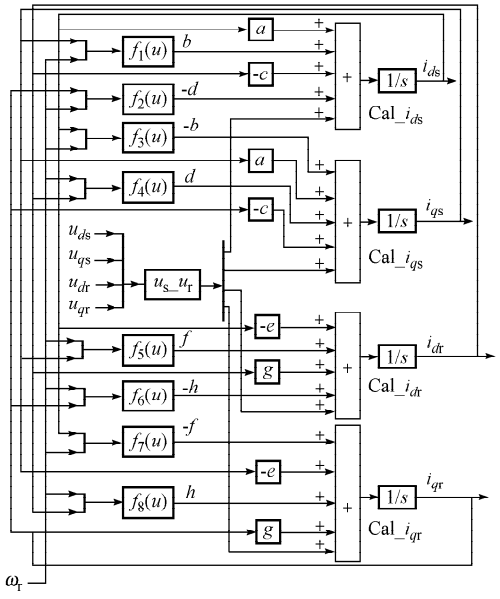

Fig. 4 Detailed generator structure in the 8th and 5th order models

Fig. 5 depicts the detailed structure of the drive train in the 8th order model. In Fig. 5, the electromagnetic torque T_G is calculated according to equation (6) and the gain $K_1 = 1.5 n_p L_m$. In the block "Cal_ω_r", the electrical angular speed ω_r is calculated based on the state-space model of the drive train that is represented by equation (3).

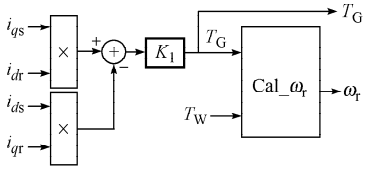

Fig. 5 Drive train structure in the 8th order model

The drive train structure in the 5th order model is shown in Fig. 6, which can be explained by equation (11). In the figure, $K_2 = D$ and $K_3 = n_p / J_{eq}$.

The overall structure of the 3rd order model of DFIG wind turbine is shown in Fig. 7. As analyzed in Section 2.3, the block "DriveTr" in Fig. 7 is used to calculate the electrical angular speed ω_r based on equations (9), (10) and (17).

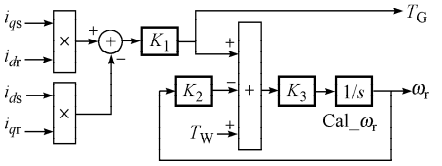

Fig. 6 Drive train structure in the 5th order model

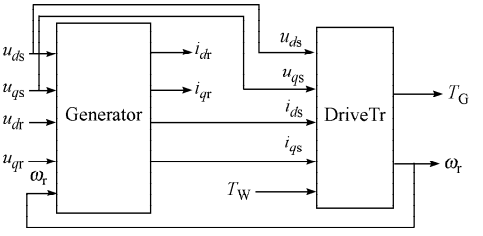

Fig. 7 Overall structure of the 3rd order model

The block "Generator" in Fig. 7 is illustrated in detail by Fig. 8, where, "Cal_i_{dqs}" functions to calculate i_{ds} and i_{qs} based on equations (5), (13) and (14), "Cal_i_{dqr}" to calculate i_{dr} and i_{qr} according to equation (13), "Cal_e_d" and "Cal_e_q" to calculate e_d and e_q respectively according to equation (16).

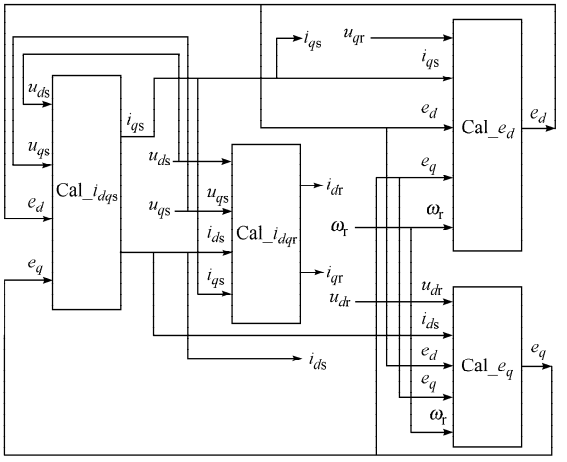

Fig. 8 Detailed generator structure in the 3rd order model

4 Simulation and Analysis

In order to validate the models and compare their dynamic behaviors, simulations for the wind speed changes and the rotor voltage adjustment are performed on MATLAB/Simulink. Analysis and comparisons of the simulation results will hopefully contribute to deeply understanding the dynamic performances of each type of the models and choosing an appropriate one for specific studies as well.

A DFIG of 200 kW, 4 poles, 690 V is used and the machine parameters are as follows: $f = 50$ Hz, $R_s = 0.093\ 4\ \Omega$, $R_r = 0.094\ 2\ \Omega$, $L_{sk} = 0.000\ 53$ H, $L_{rk} = 0.000\ 56$ H, $L_m = 0.025\ 17$ H, $J_G = 5$ kg·m^2, $J_W =$

15 000 kg·m², R=17 m, k=70 000 (N·m)/rad, n_g=30, γ=7, the corresponding power coefficient C_p=0.41, the friction coefficient D=0.02. Two cases have been simulated to verify and compare the models. In the simulation, electrical angular speed ω_r and electromagnetic torque T_G are displayed for each model.

Case 1: at t=8 s, as the wind speed increases, ω_r has to go up from 343 rad/s to 365 rad/s. In this case, the two axis components of the stator voltage are u_{ds}=0, u_{qs}=398 V. The simulation results are shown in Fig. 9 ~ Fig. 11.

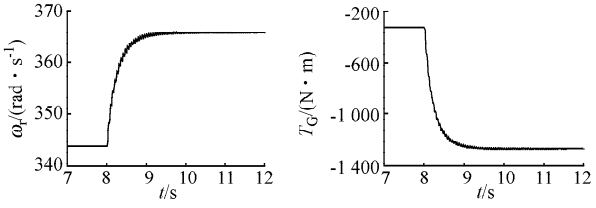

Fig. 9 Simulation results of the 8th order model in Case 1

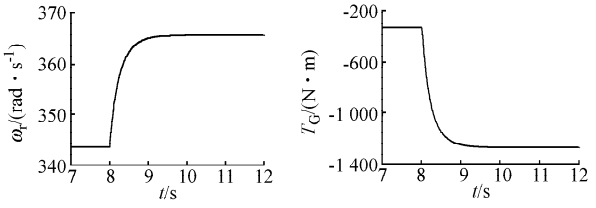

Fig. 10 Simulation results of the 5th order model in Case 1

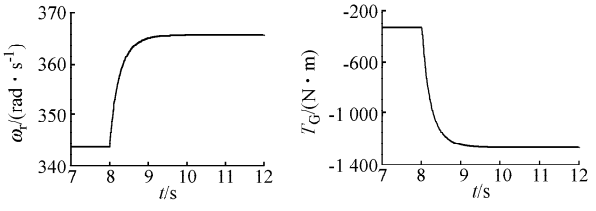

Fig. 11 Simulation results of the 3rd order model in Case 1

Case 2: at t=8 s, there is a 30% dip (from 398 V to 278 V) in the stator voltage. After 0.3 s, the voltage recovers to the value of 398 V. In this case, the wind speed remains unchanged at 7 m/s. In order to compare the dynamic performances of different models, the two axis components of the rotor voltage remain unchanged, Specifically, u_{dr}=4.7 V, u_{qr}=−30 V. The simulation results are shown in Fig. 12 ~ Fig. 14.

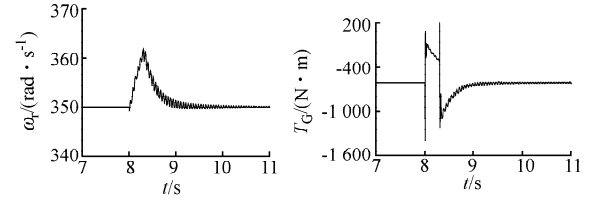

Fig. 12 Simulation results of the 8th order model in Case 2

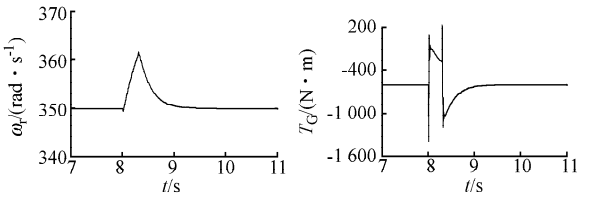

Fig. 13 Simulation results of the 5th order model in Case 2

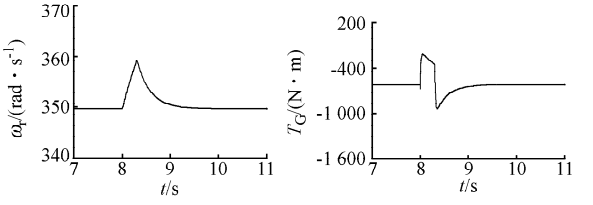

Fig. 14 Simulation results of the 3rd order model in Case 2

The simulation results demonstrate that the models provide very similar responses to external disturbances. But the 8th order model displays the phenomenon of torsional oscillation, which can be credited to the inclusion of flexibility of the drive train. Therefore, this type of model is more suitable for investigating the torsion related problems. The 5th order model provides very similar results with those of its 8th order counterpart. In Case 2, the change of the electrical torque of the 3rd order model is much slighter than any of the other models. This is mainly caused by neglection of the electromagnetic transients in the stator.

The simulation of the two cases is conducted on a 1.6 GHz personal computer. The simulation times for the three types of model are given in Table 1, where, t_{sim1} is the simulation time in Case 1 (from 7 s to 12 s) and t_{sim2} is the simulation time in Case 2 (from 7 s to 11 s) respectively. Apparently, the 3rd order model is the most time-effective. So, this model is more suitable for studying complex power systems when taking into account the characteristics of DFIG.

Table 1 Simulation time comparisons

model types	t_{sim1}/s	t_{sim2}/s
8th order	0.100	0.182
5th order	0.023	0.063
3th order	0.017	0.061

5 Conclusion

The 8th, 5th and 3rd order models of DFIG wind turbine are described in the paper. The three types of models are simulated in MATLAB/Simulink software package and two scenarios are studied. The simulation results exhibit a good agreement between different models. However, the responses of the 8th order model reveal the nature of the complete drive train dynamics, but with the slowest simulation speed. When the problems, such as torsional fatigue, are studied, this model is more reliable than the other two. Although the 3rd order model is very largely

approximate, its result is acceptable in precision and its simulation is the fastest. Therefore, this model is appropriate for the study of large power systems with DFIG wind turbines connected. It is noteworthy that the 5th order model describes the behavior of the generator in more details with the transients on both the stator and rotor side reflected, and the simulation speed is fast enough for most studies.

References

[1] LEI Yazhou, LIGHTBODY G. Wind energy and electricity market. Automation of Electric Power Systems (Chinese), 2005, 29(10): 1-5.

[2] LEI Yazhou. Studies on wind farm integration into power system. Automation of Electric Power Systems (Chinese), 2003, 27(8): 84-89.

[3] MULLER S, DEICKE M, DE DONCKER R W. Doubly fed induction generator systems for wind turbines. IEEE Industry Applications Magazine, 2002, 8(3): 26-33.

[4] SALMAN S K, ANITAL J T. Windmill modeling consideration and factors influencing the stability of a grid-connected wind power-based embedded generator. IEEE Trans on Power Systems, 2003, 18(2): 793-802.

[5] HE Yikang, ZHENG Kang, PAN Zaiping, et al. Investigation on an AC excited variable-speed constant-frequency wind-power generation system. Automation of Electric Power Systems (Chinese), 2004, 28(13): 55-59.

[6] PETRU T, THIRINGER T. Modeling of wind turbines for power system studies. IEEE Trans on Power Systems, 2002, 17(4): 1132-1139.

[7] EKANAYAKE J B, HOLDSWORTH L, JENKINS N. Comparison of 5th order and 3rd order machine models for doubly fed induction generator (DFIG) wind turbines. Electric Power Systems Research, 2003, 67(3): 207-215.

[8] PARATHANASSIOU S A, PAPADOPOULOS M P. Dynamic behavior of variable speed wind turbines under stochastic wind. IEEE Trans on Energy Conversion, 1999,14(4): 1617-1632.

[9] LI Dongdong, CHEN Chen. A study on dynamic model of wind turbine sets. Proceedings of the CSEE (Chinese), 2005, 25(3): 115-119.

[10] WU Xiaojie, CHAI Jianyuan, WANG Xiangheng. Overview of AC excitation for variable speed constant frequency double fed wind power generator systems. Automation of Electric Power Systems (Chinese), 2004, 28(23): 92-96.

[11] BATTAIOTTO P E, MANTZ R J, PULESTON P F. A wind turbine emulator based on a dual DSP process. Control Engineering Practice, 1996, 4(9): 1261-1266.

[12] SHALTOUT A A, EL-RAMAHI A F. Maximum power tracking for a wind driven induction generator connected to a utility network. Applied Energy, 1995, 52(2-3): 243-253.

[13] SONG Y D, DHINAKARAN B, BAO X Y. Variable speed control of wind turbines using nonlinear and adaptive algorithms. Journal of Wind Engineering and Industrial Aerodynamics, 2000, 85(3): 293-308.

[14] SUN T, CHEN Z, BLAABJERG F. Voltage recovery of grid-connected wind turbines after a short-circuit fault// Proceedings of the 29th Annual Conference of the IEEE Industrial Electronics Society: Vol 3, Nov 2-6, 2003, Roanoke, VA, USA. Los Alamitos, CA, USA: IEEE Computer Society, 2003: 2723-2728.

YIN Ming(1974—), male, was born in Hebei Province, China. He received the B. S. degree in Power System and Its Automation from North China Electric Power University (NCEPU) in 1996. He is currently pursuing his Ph. D. degree at NCEPU. His research interests include HVDC, wind power technology and flexible AC transmission system (FACTS).

LI Gengyin (1964—), male, was born in Hebei Province, China. He received the B. S., M. S. and Ph. D. degrees, all in Electrical Engineering, from North China Electric Power University (NCEPU) in 1984, 1987 and 1996, respectively. Since 1987, he has been with the Department of Electrical Engineering at NCEPU, where he is currently a professor and deputy head of the Department. His research interests include power quality, electricity markets, and new transmission and distribution technologies. E-mail: ligy@ncepu. edu. cn

ZHOU Ming(1967—), female, was born in Hubei Province, China. She received the B. S., M. S. and Ph. D. degrees in Electrical Engineering from North China Electric Power University (NCEPU) in 1989, 1992 and 2006, respectively. Since 1992, she has been with the Department of Electrical Engineering at NCEPU, where she is currently an associate professor. Her research interests include electricity markets, power quality, AI applications to power systems, and power system operation and management.

双馈感应风力发电机组动态模型的分析与比较

尹 明，李庚银，周 明，赵成勇

（华北电力大学电力系统保护与动态安全监控教育部重点实验室，河北省保定市 071003）

摘要：在大型风力发电厂中双馈感应风力发电机组将被广泛应用，深入了解双馈感应风力发电机组动态特性非常必要。文中给出了双馈机组的8阶、5阶和3阶模型。8阶模型包括完整的传动系统模型、定子模型和转子模型；5阶模型包括定子、转子模型和简化的传动系统模型；忽略定子的暂态过程后，3阶模型包括转子模型和简化的传动系统模型。在MATLAB/Simulink软件上实现了3种模型建模。完成了对2种情况的仿真，仿真结果验证了上述3种模型的正确性，并比较了各自的响应特性。仿真结果表明：8阶模型具有最精确完整的响应，但仿真时间最长；3阶模型采用最大程度的近似，但仿真时间最短；5阶模型适合大多数既要求较快仿真速度又要求较高精度的研究。

关键词：双馈感应发电机；风力发电；动态模型；变速风力机